

Longitudinal scaling of observables in heavy-ion collision models

Md. Nasim¹, Chitrasen Jena², Lokesh Kumar³, Pawan Kumar Netrakanti⁴ and Bedangadas Mohanty¹

¹Variable Energy Cyclotron Centre, Kolkata 700064, India, ²Institute of Physics, Bhubaneswar 751001, India, ³Kent State University, Kent, Ohio 44242, USA, and ⁴Bhabha Atomic Research Centre, Mumbai 400 085, India
(Dated: January 19, 2013)

Longitudinal scaling of pseudorapidity distribution of charged particles ($dN_{\text{ch}}/d\eta$) is observed when presented as a function of pseudorapidity (η) shifted by the beam rapidity ($\eta - y_{\text{beam}}$) for a wide range of collision systems ($e^+ + e^-$, $p+p$, $d+A$ and $A+A$) and beam energies. Such a scaling is also observed for the elliptic flow (v_2) of charged hadrons in $A+A$ collisions. This is a striking observation, as v_2 is expected to be sensitive to the initial conditions, the expansion dynamics and the degrees of freedom of the system, all of which potentially varies with collision system and colliding energies. We present a study of the longitudinal scalings of $dN_{\text{ch}}/d\eta$, average transverse momentum ($\langle p_T \rangle$) and v_2 using transport models UrQMD and AMPT for Au+Au collisions at center of mass energies ($\sqrt{s_{\text{NN}}}$) of 19.6, 62.4, 200 GeV and Pb+Pb collisions at 2760 GeV. Only the AMPT models which includes partonic effects and quark coalescence as a mechanism of hadronization, shows longitudinal scaling for $dN_{\text{ch}}/d\eta$, $\langle p_T \rangle$ and v_2 . Whereas the UrQMD and AMPT default versions show longitudinal scaling only for $dN_{\text{ch}}/d\eta$ and $\langle p_T \rangle$. We also discuss the possibility of longitudinal scaling of v_2 within two extreme scenarios of models with hydrodynamic and collisionless limits. We find the longitudinal scaling of bulk observables to be an important test for the underlying physics mechanism in models of particle production.

PACS numbers: 25.75.Ld

I. INTRODUCTION

Scale invariance in experimental observables from heavy-ion collisions at the Relativistic Heavy Ion Collider have provided interesting insights about particle production mechanism in these reactions [1]. Observables like $\langle p_T \rangle$, freeze-out parameters [2], pion interferometry radii [3] are observed to scale with some powers of $dN_{\text{ch}}/d\eta$. Within the frame work of thermal models some of these reflect a constant energy per particle at freeze-out. The elliptic flow for identified baryons and mesons when divided by the number of constituent quarks is found to scale with the kinetic energy of the particles (or constituents) [4]. This has been interpreted as due to development of substantial collectivity in the partonic phase [5] of the evolution of the heavy-ion collisions and coalescence being the dominant mechanism of particle production for the intermediate p_T range of 2 - 6 GeV/c [6]. Scalings have been observed in $p+p$ collisions. At low p_T (< 2 GeV/c) for a given \sqrt{s} , the invariant yields of identified hadrons are observed to scale when plotted as a function of m_T ($m_T = \sqrt{p_T^2 + m^2}$ and m is the mass of the hadron), [7]. This indicates the absence of significant radial flow in $p+p$ collisions. At high p_T (> 2 GeV/c) the product of the invariant yields of a hadron and some power of the \sqrt{s} become independent of \sqrt{s} when plotted as a function of x_T ($= 2p_T/\sqrt{s}$) [8]. This is interpreted as due to dominance of the pQCD process (jets) in $p+p$ collisions. Scaling has been also observed in the longitudinal direction, represented

by a variable $\eta - y_{\text{beam}}$, in $dN_{\text{ch}}/d\eta$ [9], v_2 [10] and directed flow (v_1) [11] in $A+A$ collisions. Further such scaling have been widely used to predict the values of the observables at higher energy regimes in nucleus-nucleus collisions [12]. Recent results on $dN_{\text{ch}}/d\eta$ at midrapidity for Pb+Pb central collisions at $\sqrt{s_{\text{NN}}} = 2760$ GeV is found to be higher than expected from extrapolation based on the longitudinal scaling of $dN_{\text{ch}}/d\eta$ at lower beam energies [13].

The longitudinal scaling of $dN_{\text{ch}}/d\eta$ is a widely discussed subject as it is observed for variety of colliding systems starting from $e^+ + e^-$, $p+p$, $d+A$ to $A+A$ collisions [9, 14]. This phenomena is often called limiting fragmentation. It was hypothesized by Benecke et al. [15], Feynman [16] and Hagedron [17] that as $\sqrt{s} \rightarrow \infty$ the multiplicity distribution becomes independent of \sqrt{s} . From a microscopic picture the longitudinal scaling is understood. assuming the rapidity distributions of the produced particles are functions of x (fraction of the hadron longitudinal momentum carried by a typical parton) alone, and not of the total energy. If the hadron interactions are short-ranged in rapidity then the hadron rapidity distributions would reproduce the corresponding distributions of the liberated partons. The picture is very similar to Bjorken scaling of parton distributions. This interpretation can be easily linked to initial state gluon dynamics of the system [18]. From a macroscopic picture, the entropy conservation in heavy-ion collisions can make $dN_{\text{ch}}/d\eta$ insensitive to some aspects of dynamics of system and hence may be the cause of the scaling.

The p_T integrated v_2 for a given rapidity range is defined as [19]

$$v_2 = \langle \cos(2(\phi - \Psi)) \rangle, \quad (1)$$

where ϕ and Ψ are the charged particle azimuthal angle and reaction plane angle respectively. The observed v_2 is affected by the initial conditions, it is sensitive to the equation of state and its magnitude is determined by the interactions of the constituents through out the evolution of the system in heavy-ion collisions [20, 21]. Hence the physical interpretation of longitudinal scaling of v_2 is counter intuitive. Longitudinal scaling of v_2 exhibited for a wide beam energy range, different collision centrality and collision species would tend to indicate weak dependence of v_2 on the above mentioned physical conditions. Recent studies [21] suggest that the simultaneous observation of longitudinal scaling of v_2 and $dN_{ch}/d\eta$ can be reconciled only if the system formed in heavy-ion collisions are weakly coupled. This is contrary to other indirect estimations of the shear viscosity to entropy ratio which suggests the system is strongly coupled [22].

In this paper, we study the longitudinal scaling of $dN_{ch}/d\eta, \langle p_T \rangle$ and v_2 using models AMPT (A Multi Phase Transport Model, ver 1.11) [23] and UrQMD (Ultra Relativistic Quantum Molecular Dynamics, ver 2.3) [24] for charged particles in Au+Au collisions at $\sqrt{s_{NN}} = 19.6, 62.4, 200$ GeV and Pb+Pb collisions at $\sqrt{s_{NN}} = 2760$ GeV. The aim being to see if these models also exhibit such longitudinal scalings and hence provide a physical insight behind the phenomena. The UrQMD model is based on a microscopic transport theory where phase space description of the reactions and hadron-hadron interactions are important. The AMPT model can be studied in two configurations, in the AMPT default version the minijet partons are made to undergo scattering before they are allowed to fragment into hadrons, while in the AMPT-SM string melting scenario additional scattering occurs among the quarks and the hadronization occurs through the mechanism of parton coalescence.

II. LONGITUDINAL SCALING OF $dN_{ch}/d\eta$ AND $\langle p_T \rangle$

Figure 1 shows the $dN_{ch}/d\eta$ versus $\eta - y_{beam}$ for 0–6% central Au+Au collisions at $\sqrt{s_{NN}} = 19.6, 62.4$ and 200 GeV from (a) the PHOBOS experiment at RHIC [9], (b) UrQMD, (c) AMPT and (d) AMPT-SM models. Also shown are the results from the models for Pb+Pb collisions at $\sqrt{s_{NN}} = 2760$ GeV. The y_{beam} values for $\sqrt{s_{NN}} = 19.6, 62.4, 200$ and 2760 GeV are 3.03, 4.19, 5.36 and 7.98 respectively. The longitudinal scaling observed in $dN_{ch}/d\eta$ in the

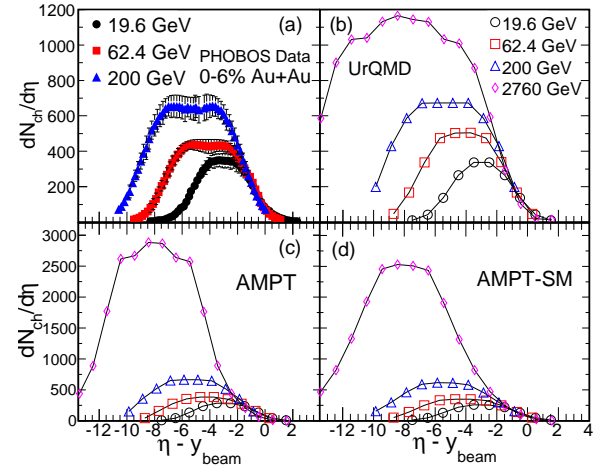


FIG. 1: (Color online) $dN_{ch}/d\eta$ versus $\eta - y_{beam}$ for 0–6% central Au+Au collisions at $\sqrt{s_{NN}} = 19.6, 62.4$ and 200 GeV from (a) the PHOBOS experiment at RHIC [9], (b) UrQMD, (c) AMPT default and (d) AMPT-SM. Also shown are the model results from Pb+Pb collisions at $\sqrt{s_{NN}} = 2760$ GeV.

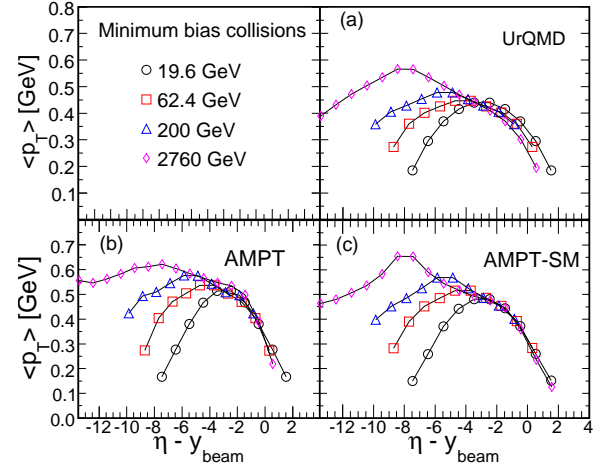


FIG. 2: (Color online) $\langle p_T \rangle$ versus $\eta - y_{beam}$ for minimum bias Au+Au collisions at $\sqrt{s_{NN}} = 19.6, 62.4$ and 200 GeV from (a) the UrQMD, (b) AMPT default and (c) AMPT-SM. Also shown are the model results from Pb+Pb collisions at $\sqrt{s_{NN}} = 2760$ GeV.

data (Fig. 1(a)) is also observed in all the models studied. Such scalings have also been observed for other models like HIJING [25] and HIJING B \bar{B} [26, 27].

Figure 2 shows the $\langle p_T \rangle$ for the charged particles versus $\eta - y_{beam}$ for minimum bias Au+Au collisions at $\sqrt{s_{NN}} = 19.6, 62.4$ and 200 GeV from (a) the UrQMD, (b) AMPT and (c) AMPT-SM models. Also shown are the results from the models for min-

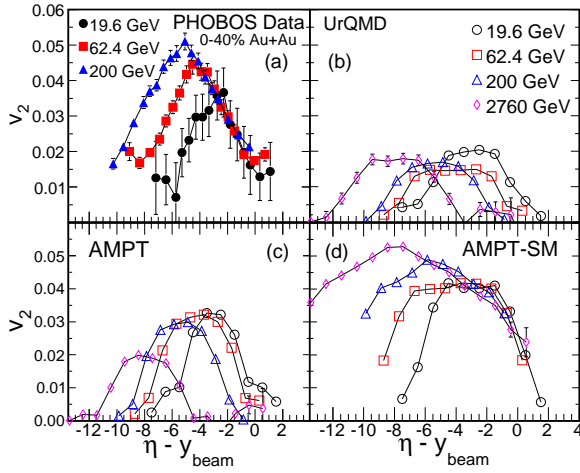


FIG. 3: (Color online) v_2 for charged particles versus $\eta-y_{\text{beam}}$ for 0–40% central Au+Au collisions at $\sqrt{s_{\text{NN}}} = 19.6, 62.4$ and 200 GeV from (a) the PHOBOS experiment at RHIC [10], (b) UrQMD, (c) AMPT default and (d) AMPT-SM. Also shown are the model results from Pb+Pb collisions at $\sqrt{s_{\text{NN}}} = 2760$ GeV.

imum bias Pb+Pb collisions at $\sqrt{s_{\text{NN}}} = 2760$ GeV. There are no experimental data available at RHIC for $\langle p_T \rangle$ versus $\eta-y_{\text{beam}}$ hence not shown in the figure. The longitudinal scaling is observed in all the models studied.

These results then sets the stage for studying the longitudinal scaling in v_2 . Note that the goal here is not to have a quantitative comparison with data on the scalings in $dN_{\text{ch}}/d\eta$ and v_2 , but to see if the observations are qualitatively reproduced in the models.

III. LONGITUDINAL SCALING OF v_2

Figure 3 shows the v_2 for charged particles versus $\eta-y_{\text{beam}}$ in Au+Au collisions at $\sqrt{s_{\text{NN}}} = 19.6, 62.4$ and 200 GeV [10]. The results from the models for Pb+Pb collisions at $\sqrt{s_{\text{NN}}} = 2760$ GeV are also shown. The collision centrality is 0–40% central and is different for that shown for $dN_{\text{ch}}/d\eta$ in Fig. 1. The choice of centrality is based on availability of the v_2 data for charged particles in the experiment as a function of rapidity. Figure 3 (a) shows the longitudinal scaling of v_2 as measured by the PHOBOS experiment [10]. Fig. 3 (b) shows the v_2 vs. $\eta-y_{\text{beam}}$ from UrQMD model, in (c) the corresponding results from AMPT default are shown and in (d) the same results from AMPT-SM are presented. It is observed that the UrQMD and the AMPT default models do not show the longitudinal scaling as observed in the data (Fig. 3 (a)). Only the AMPT

model with string melting qualitatively reproduces the observed longitudinal scaling of v_2 .

IV. DISCUSSIONS

It is worthwhile to now discuss briefly the differences in these transport models. The main difference between UrQMD and AMPT lies in the initial conditions (for AMPT taken from HIJING [25]) and additional initial state rescatterings in AMPT. The main difference between AMPT default and AMPT-SM lies in the following: The string melting version of the AMPT model is formulated on the idea that for energy densities beyond a critical value of $\sim 1 \text{ GeV}/fm^3$, it is difficult to visualize the coexistence of strings (or hadrons) and partons. Hence the need to melt the strings to partons. This is done by converting the mesons to a quark and anti-quark pair, baryons to three quarks etc. The scattering of the quarks are then carried out based on parton cascade [23]. The parton-parton cross section taken here is 10 mb. Once the interactions stop, the partons then hadronizes through the mechanism of partonic coalescence. While for the AMPT default the scattering occurs for minijet partons (no melting of strings to partons) and hadronization occurs through fragmentation process [28]. This model based study then suggests that partonic interactions in high energy density matter is essential to qualitatively reproduced the simultaneous observation of the longitudinal scalings in $dN_{\text{ch}}/d\eta$ and v_2 in experiment. If this is the actual cause then it will be interesting to have experimental measurements of v_2 vs. η for lower beam energies where we do not expect to create a sufficiently high energy density system to see the breakdown of such a v_2 longitudinal scaling.

We now briefly discuss some other possibilities which could explain the longitudinal scaling of v_2 . One of them is based on the arguments whether the system is weakly coupled or strongly coupled. A weakly coupled system has been argued to favor the combined v_2 and $dN_{\text{ch}}/d\eta$ scaling behavior [21]. It has been suggested that for systems where the interactions among the constituent particles are small, or the system is close to free streaming, called the collisionless limit [29], the $v_2 \sim \frac{dN}{d\eta} \frac{\langle v\sigma \rangle}{\pi R_x R_y}$. Where v is the relative velocity of the particles, σ is the momentum transfer interaction cross section and the product $\pi R_x R_y$ is the transverse overlap area for the two nuclei. In this model, one can easily see that v_2 should exhibit a longitudinal scaling similar to $dN_{\text{ch}}/d\eta$ provided $\langle v\sigma \rangle$ does not change with beam energy. A linear dependence of v_2 with change in $\frac{1}{\pi R_x R_y} \frac{dN}{d\eta}$ has been observed in experiments over a wide collision systems [30]. In the event of $\langle v\sigma \rangle$ changing with beam energy, possibly due to change

in the relevant degrees of freedom (hadronic or partonic), there would be a breakdown of the longitudinal scaling of v_2 . This is consistent with the conclusions from our model study. Now let us move to the other extreme limit, where the rescattering among the constituent particles are abundant leading to the hydrodynamic limit [29]. In such a model the v_2 is proportional to the average transverse momentum of the particles among several other quantities as discussed in [19]. If the $\langle p_T \rangle$ also exhibits a longitudinal scaling then v_2 in the hydrodynamic limit scenario should also exhibit the scaling. Measuring $\langle p_T \rangle$ vs. η could help address the cause of the longitudinal scaling of v_2 . However we have seen in Fig. 2 that the models based on transport approach also exhibit longitudinal scaling of $\langle p_T \rangle$. The model study for all the three observables indicates that observing longitudinal scaling in $dN_{ch}/d\eta$ and/or $\langle p_T \rangle$ does not necessarily implies we should see a similar scaling in v_2 .

V. SUMMARY

In summary, we have discussed the simultaneous observation of longitudinal scaling of $dN_{ch}/d\eta$ and v_2 when plotted as a function of $\eta - y_{beam}$ in RHIC experiments in Au+Au collisions at $\sqrt{s_{NN}} = 19.6, 62.4, \text{ and } 200 \text{ GeV}$. There are several physical arguments based on conservation of entropy and hadron distributions in rapidity corresponding to the rapidity distributions of partons (assuming hadron interactions are short ranged in rapidity) to explain the longitudinal scaling of $dN_{ch}/d\eta$. The UrQMD and AMPT models qualitatively reproduce the experimental observations for the $\sqrt{s_{NN}} = 19.6 - 2760 \text{ GeV}$. These models also exhibit longitudinal scaling in $\langle p_T \rangle$. The observation of longitudinal scaling for v_2 which could be sensitive to several quantities like initial conditions/densities, equation of state and rescatterings among the constituents is bit in-

triguing. We find that among the models studied, only AMPT with string melting qualitatively shows the behaviour as exhibited by the data. The main difference between this version of the AMPT model compared to the default version and UrQMD lies in the partonic interactions and hadronization through coalescence mechanism. We also discussed that the longitudinal scaling can naturally occur for a system in the collisionless limit. In such a limit v_2 proportional only to $dN_{ch}/d\eta$ provided the product of interaction cross section and average relative velocity of the particles does not change with the beam energy studied. It is expected that the interaction cross sections could be very different if the relevant degrees of freedom are partonic or hadronic. So studying the longitudinal scaling of v_2 at lower and higher beam energies will provide additional insight. For the other extreme, hydrodynamic limit, since v_2 is proportional to $\langle p_T \rangle$, it would be interesting to measure in experiments the $\langle p_T \rangle$ vs. η for various beam energies. However the model study of the observables $dN_{ch}/d\eta$, $\langle p_T \rangle$ and v_2 indicates that observing longitudinal scaling in $dN_{ch}/d\eta$ and/or $\langle p_T \rangle$ does not necessarily implies that such a scaling will follow in v_2 .

Acknowledgments

We thank Dr. G. Torrieri for discussing the topic of longitudinal scaling of v_2 and his helpful suggestions. X. F. Luo for help in model data at LHC energy. Financial assistance from the Department of Atomic Energy, Government of India is gratefully acknowledged. PKN is grateful to the Board of Research on Nuclear Science and Department of Atomic Energy, Government of India for financial support in the form of Dr. K.S. Krishnan fellowship. LK is supported by DOE grant DE-FG02-89ER40531. BM is supported by the DAE-BRNS project sanction No. 2010/21/15-BRNS/2026.

-
- [1] I. Arsene et al., (BRAHMS Collaboration), Nucl. Phys. A 757, 1 (2005); B. B. Back et al., (PHOBOS Collaboration), Nucl. Phys. A 757, 28 (2005); J. Adams et al., (STAR Collaboration), Nucl. Phys. A 757, 102 (2005); K. Adcox et al., (PHENIX Collaboration), Nucl. Phys. A 757, 184 (2005).
 - [2] M. M. Aggarwal, et al., (STAR Collaboration), arXiv:1008.3133; B.I. Abelev, et al., (STAR Collaboration), Phys. Rev. C 79, 034909 (2009).
 - [3] B. I. Abelev, et al., (STAR Collaboration), Phys. Rev. C 80, 024905 (2009).
 - [4] B. I. Abelev, et al., (STAR Collaboration), Phys. Rev. C 81, 044902 (2010); B. I. Abelev, et al., (STAR Collaboration), Phys. Rev. C 77, 054901 (2008); A. Adare, et al., (PHENIX Collaboration), Phys. Rev. Lett 105, 062301 (2010); S. Afanasiev, et al., (PHENIX Collaboration), Phys. Rev. Lett. 99, 052301 (2007).
 - [5] STAR Collaboration, B. I. Abelev *et al.*, Phys. Rev. Lett. **99**, 112301 (2007).
 - [6] D. Molnar and S. A. Voloshin, Phys. Rev. Lett. **91**, 092301 (2003).
 - [7] B. I. Abelev, et al., (STAR Collaboration), Phys. Rev. C 75, 064901 (2007); B. I. Abelev, et al., (STAR Collaboration), Phys. Rev. C 78, 044906 (2008).

- [8] J. Adams, et al., (STAR Collaboration), Phys. Lett. B **637**, 161 (2006).
- [9] B. Alver, et al., (PHOBOS Collaboration), Phys. Rev. Lett **102**, 142301 (2009); B. B. Back, et al., (PHOBOS Collaboration), Phys. Rev. Lett **91**, 052303 (2003); J. Adams, et al. (STAR Collaboration), Phys. Rev. Lett **95**, 062301 (2005); J. Adams, et al. (STAR Collaboration), Phys. Rev. **C 73**, 034906 (2006). B. I. Abelev, et al., (STAR Collaboration), Nucl. Phys. A **832**, 134 (2010).
- [10] B. B. Back, et al., (PHOBOS Collaboration), Phys. Rev. Lett **94**, 122303 (2005).
- [11] B. B. Back, et al., (PHOBOS Collaboration), Phys. Rev. Lett **97**, 012301 (2006).
- [12] N. Armesto, (ed.) et al., J. Phys. G **35**, 054001 (2008).
- [13] K. Aamodt, et al., (ALICE Collaboration), Phys. Rev. Lett **97**, 252301 (2010).
- [14] B. B. Back, et al., (PHOBOS Collaboration), Phys. Rev. C **74**, 021902(R) (2006); B. B. Back, et al., (PHOBOS Collaboration), Phys. Rev. C **72**, 031901(R) (2005).
- [15] J. Benecke, T. T. Chou, C. N. Yang, and E. Yen, Phys. Rev. **188**, 2159 (1969).
- [16] R. P. Feynman, Phys. Rev. Lett. **23**, 1415 (1969).
- [17] R. Hagedorn, Nucl. Phys. B **24**, 93 (1970).
- [18] E. Iancu, Nucl. Phys. A **715**, 219 (2003); S. Jeon, V. T. Pop and M. Bleicher, Phys. Rev. C **69**, 044904 (2004).
- [19] S. Voloshin, Y. Zhang, Z. Phys. **C 70**, 665 (1996); S. A. Voloshin, A. M. Poskanzer and R. Snellings, arXiv:0809.2949.
- [20] J. Y. Ollitrault, Phys. Rev. **D 46**, 229 (1992); H. Sorge, Phys. Rev. Lett. **78**, 2309 (1997). P. Huovinen, P. F. Kolb, U. Heinz, P. V. Ruuskanen, and S.A. Voloshin, Phys. Lett. **B503**, 58 (2001).
- [21] G. Torrieri, Phys. Rev. C **82**, 054906 (2010).
- [22] R. A. Lacey, et al., Phys. Rev. Lett. **98**, 092301 (2007); S. Gavin and M. Abdel-Aziz, Phys. Rev. Lett. **97**, 162302 (2006); A. Adare, et al., (PHENIX Collaboration) Phys. Rev. Lett. **98**, 172301 (2007); H.-J. Drescher, A. Dumitru, C. Gombeaud and J.-Y. Ollitrault, Phys. Rev. C **76**, 024905 (2007).
- [23] Zi-Wei Lin, C. M. Ko, Phys. Rev. **C 65**, 034904 (2002); Zi-Wei Lin *et al.*, Phys. Rev. **C 72**, 064901 (2005).
- [24] S. A. Bass *et al.*, Prog. Part. Nucl. Phys. **41** 255 (1998); M. Bleicher *et al.*, J. Phys. G **25** 1859 (1999).
- [25] X. N. Wang and M. Gyulassy, Phys. Rev. D **44**, 3501 (1991).
- [26] S. E. Vance, M. Gyulassy and X. N. Wang, Phys. Lett. B **443**, 45 (1998); S. E. Vance and M. Gyulassy, Phys. Rev. Lett. **83**, 1735 (1999).
- [27] Pawan Kumar Netrakanti, Ph. D thesis, Jadavpur University, 2006.
- [28] B. Andersson, G. Gustafson, G. Ingelman and T. Sjostrand, Phys. Rep. **97**, 31 (1983).
- [29] H. Heiselberg and A. M. Levy, Phys. Rev. C **59**, 2716 (1999).
- [30] C. Adler, et al., (STAR Collaboration), Phys. Rev. C **66**, 034904 (2002).